

Nanoscale Molecular Transport: The Case of Dip-Pen Nanolithography<sup>†</sup>Louise R. Giam,<sup>‡,§,||</sup> Yuhuang Wang,<sup>‡,§,||,#</sup> and Chad A. Mirkin<sup>\*,§,§,||</sup>*Department of Materials Science and Engineering, Department of Chemistry, International Institute for Nanotechnology, Northwestern University, 2145 Sheridan Road, Evanston, Illinois 60208-3113**Received: October 13, 2008; Revised Manuscript Received: December 12, 2008*

In dip-pen nanolithography experiments, many groups have observed that different tips deliver the same ink at different rates. This article presents a quantitative model for understanding this phenomenon and, importantly, a way of controlling it. An inkjet printer is used to deliver controlled amounts of 16-mercaptohexadecanoic acid (MHA) to atomic force microscope tips in an array. Ink transport from each tip is studied as a function of the number of drops delivered. We show a nonlinear dependence of transport rates on the number of drops that arises from surface-area-dependent dissolution of MHA. From this work, MHA dissolution attempt frequencies were calculated to be between  $1.3 \times 10^9$  and  $4.4 \times 10^9$  Hz.

Molecular transport and dissolution govern many processes, including nanolithography,<sup>1</sup> pharmaceutical activity,<sup>2</sup> and catalysis.<sup>3</sup> In our work involving the nanofabrication technique known as dip-pen nanolithography (DPN), molecular transport and dissolution are two of the key factors that govern the technology and allow one to control it.<sup>1</sup> DPN is a scanning-probe-lithography-based technique whereby a sharp atomic force microscope (AFM) tip is used to deliver a wide range of “ink” materials, including small organic molecules,<sup>4</sup> polymers,<sup>5</sup> biomolecules,<sup>6</sup> colloidal nanoparticles,<sup>7</sup> and sols,<sup>8</sup> to a surface of interest with high registry for generating nanoscale features in a constructive manner.<sup>9</sup> Humidity and the water meniscus that forms between tip and substrate are important factors that influence transport rate. DPN has enabled many fundamental studies involving molecular transport,<sup>10</sup> adsorbate self-organization and migration,<sup>11</sup> and the role of the water meniscus in scanning probe lithographies.<sup>12</sup> It also has proven to be a useful tool for making and studying highly miniaturized structures, including nanoelectronic devices, DNA and protein arrays, and chemical and biological sensors.<sup>9,13</sup> One of the proposed mechanisms for DPN involves transport of ink molecules through a water meniscus formed between the AFM tip and substrate due to capillary condensation.<sup>14</sup> More specifically, DPN transport models typically assume that the tip coated with an alkanethiol (e.g., 16-mercaptohexadecanoic acid, MHA) is a point source of constant concentration<sup>12</sup> or flux.<sup>13</sup> Although a constant point source model explains the time-dependent growth of MHA patterns for a single ink-coated tip, the variation of transport rates among different tips or for different ink coating methods has been ignored, despite its importance to forming a complete understanding of material transport. Such an understanding would allow one to significantly increase the reproducibility<sup>10</sup> of DPN and aid in parallelization efforts,<sup>15</sup> where one must be able to achieve uniform and nearly identical transport rates from different pens in an array. In this article, we describe

a quantitative model accounting for the variation in DPN transport rates and a method for controlling them.

Using a noncontact piezoelectric-controlled Perkin-Elmer Piezorray inkjet printer,<sup>15</sup> 7-pen Si<sub>x</sub>N<sub>y</sub> cantilever arrays with 150 μm pen-to-pen spacing (NanoInk, Skokie, IL) were inked with 320 pL droplets of a 10 mM MHA–ethanol solution (Figure 1a, b). These inked pens were subsequently used to generate MHA self-assembled monolayer (SAM) patterns on freshly prepared polycrystalline Au substrates (Figure 1c). The Au substrates were prepared by thermal evaporation of 5 nm of Ti as an adhesion layer and 25 nm of Au on Si wafers at a rate of 1 Å/s and a base pressure of  $\leq 3 \times 10^{-6}$  Torr. DPN was performed in contact mode at a relative humidity of  $45 \pm 3\%$  and  $24 \pm 1$  °C using a NanoInk NScriptor or Veeco/Thermomicroscopes CP-III AFM. Patterns were characterized using AFM and lateral force microscopy (LFM) with a scan rate of 4 Hz. Tapping mode experiments for measuring MHA topology on flat Si<sub>x</sub>N<sub>y</sub> substrates were conducted using a Digital Instruments Multimode AFM.

Figure 2a shows the linear dependence of dot feature areas on dwell times for each set of droplet experiments. As with previously reported DPN experiments, the transport or deposition rate,  $D$ , can be determined by measuring dot pattern areas,  $P$ , as a function of dwell time,  $t$ , and the effective tip area in contact with the meniscus,  $b$ , where  $P = Dt + b$ . These functions match the continuum diffusion theory in which a tip is treated as a point source of constant flux.<sup>13</sup> Importantly, we have found that the ink transport rate is a function of the amount of material on a pen and can be systematically adjusted on the basis of the number of ink droplets delivered. For pens that were inked with up to seven MHA–ethanol drops, the transport rate increased nonlinearly as the number of droplets increased, followed by saturation (Figure 2b). Mechanical breakage of MHA crystallites from the tip precluded measurement of transport rates for tips inked with over seven drops of MHA–ethanol solution. Lower transport rates could be achieved by changing the concentration of the inkjet droplet. By decreasing the ink solution concentration to 0.5–2 mM, sub-100 nm resolution was reproducibly achieved when pens were inked with single droplets (Supporting Information).

The mass-dependent ink transport rates are not entirely due to increased tip radius of curvature or residual solvent as more

<sup>†</sup> Part of the “George C. Schatz Festschrift”.

\* E-mail: chadnano@northwestern.edu.

<sup>‡</sup> Department of Materials Science and Engineering.

<sup>§</sup> Department of Chemistry.

<sup>||</sup> International Institute for Nanotechnology.

<sup>#</sup> These authors contributed equally to this work.

<sup>‡</sup> Current address: Department of Chemistry and Biochemistry, University of Maryland, College Park, MD 20742.

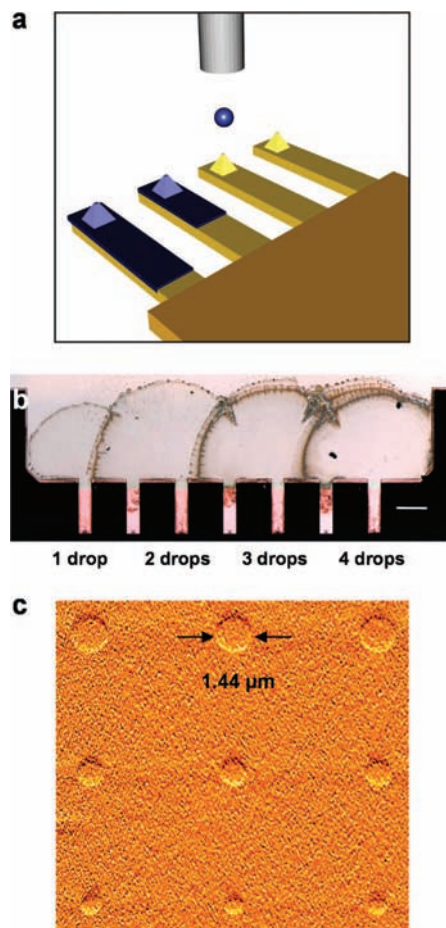


**Figure 1.** (a) Scheme of inkjet printer addressing individual tips in a cantilever array. (b) Optical microscopy image of  $\text{Si}_3\text{N}_4$  cantilevers inked with increasing drops of 10 mM MHA ethanol solution. (c) Representative error signal image (scan rate 4 Hz) of dot features formed at  $24 \pm 1$  °C with RH  $45 \pm 3\%$  on fresh Au surfaces by a tip inked with 5 drops of MHA-ethanol. From top to bottom, contact times are 16, 8, and 4 s, respectively.

ink is delivered to the tip. Indications of tip radius increase should be seen in Figure 2a, where instead of  $b$  converging, the corresponding linear fits would be offset on the  $y$ -axis. Especially for the range of 1–4 MHA-ethanol drops, the values of  $b$  are minimally affected, suggesting that there are minimal tip radii increases from more ink drops. Because  $b$  represents the tip-substrate contact area in the limit of short contact times, it is possible that meniscus formation affects the intercept values. Furthermore, the increases in transport rate were not due to residual solvent (ethanol). We found that the transport rates of inked tips with and without 18 h vacuum treatment ( $\sim 10^{-2}$  Torr) were the same.

The observation of mass-dependent ink transport rates arises from rapid depletion of MHA from the water meniscus. Although the tip is in contact with the substrate, the meniscus acts as a channel through which molecules are quickly transported to the substrate, allowing for MHA feature growth. To form a dot feature with a diameter of  $1.4 \mu\text{m}$  in 16 s (Figure 1c), however, over  $7.5 \times 10^6$  molecules are necessary, using an MHA footprint of  $0.229 \text{ nm}^2$ ,<sup>16,17</sup> far exceeding the number of MHA molecules dissolved in a saturated meniscus ( $\sim 70$  molecules, calculated from the meniscus volume at a relative humidity of 40%).<sup>14,18</sup> These values correspond to an average flux of over  $3.8 \times 10^5$  molecules  $\text{s}^{-1}$  and indicate that there is a high concentration gradient within the meniscus. Alkanethiol

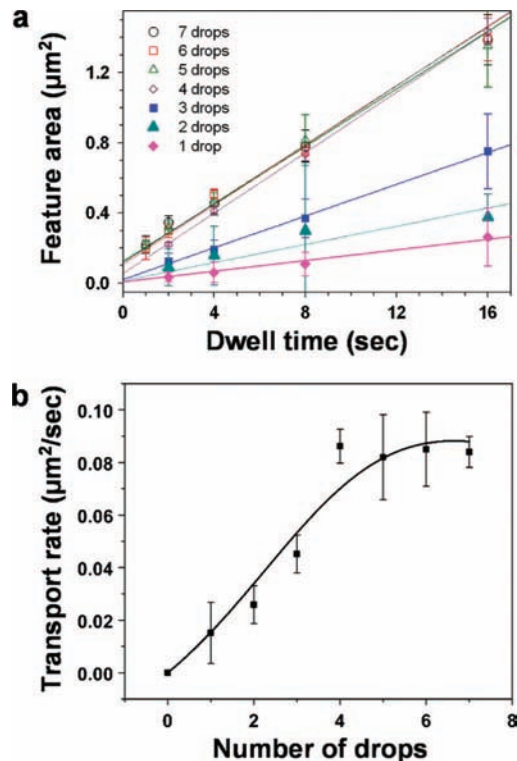


**Figure 2.** (a) Patterned MHA dot areas were measured as a function of dwell time for tips inked with increasing drops of 10 mM MHA-ethanol. All experiments were conducted at  $24 \pm 1$  °C with RH  $45 \pm 3\%$  on fresh Au substrates. For each set of inked tips, the relationship  $P = Dt + b$  can be used such that  $P$  is the feature area,  $D$  is the transport rate,  $t$  is the dwell time, and  $b$  is the effective tip area in contact with the meniscus. (b) The transport rate,  $D$ , as a function of the number of MHA-ethanol drops is fitted with a four-parameter Brunauer-Emmett-Teller (BET) equation with a constraint of passing through (0, 0). The BET equation describes multilayer adsorption.

ink transport from the meniscus to the substrate is a rapid process; an estimated bulk diffusion constant for MHA in ethanol is  $580 \mu\text{m}^2 \text{ s}^{-1}$ ,<sup>16</sup> which exceeds measured transport rates  $D$  in Figure 2b. Additionally, it has been reported that the rate constant of MHA adsorption onto a gold surface at 300 K is relatively fast at  $\sim 1.0 \times 10^3 \text{ M}^{-1} \text{ sec}^{-1}$ .<sup>16</sup> Although it remains to be confirmed whether MHA transports via the surface of the meniscus,<sup>19</sup> through the bulk,<sup>1</sup> or both, we argue that the limiting step in the transport process occurs neither at the substrate nor in the meniscus, but at the tip, the source of MHA.

To better understand the origin of mass-dependent transport rates, we deposited 10 mM droplets of MHA-ethanol on the flat  $\text{Si}_3\text{N}_4$  surface near the cantilevers and measured the topology by AFM (Supporting Information). Exposed MHA surface area  $A$  was quantified by the equation

$$A = \sum A(\Delta x, \Delta y, \Delta z) - A_0 \quad (1)$$

where  $A(\Delta x, \Delta y, \Delta z)$  represents the sum of triangulated areas formed by adjacent points on the surface, and  $A_0$  represents the projected area beneath a topological feature. Instead of a complete and homogeneous coating of MHA on the substrate, crystallites were observed. The lateral dimensions of crystallites range from nanometers to micrometers with average heights of  $\sim 100 \text{ nm}$  (Supporting Information). As with the “coffee ring” effect, in which material distribution is inhomogeneous depending on location (center vs edge of the drying footprint), surface area can change along the radial direction of the droplet footprint as well;<sup>20</sup> this phenomenon can affect transport rate if one does

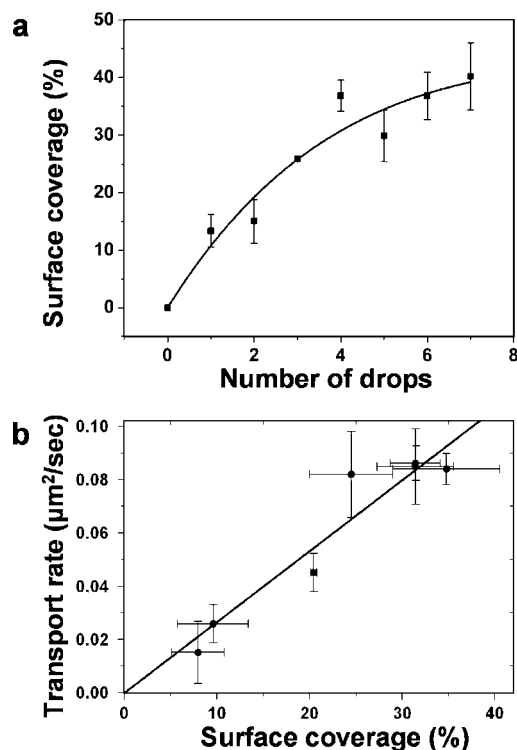


**Figure 3.** (a) Surface coverage dependence on the number of MHA–ethanol drops for  $\text{Si}_x\text{N}_y$  substrates. A line was fitted using a four-parameter BET equation with a constraint of passing through (0, 0). (b) MHA transport rate shows a linear dependence on the surface coverage and increases with the number of drops.

not inkjet droplets directly at the tip. Although the surface coverage determined from a flat surface may not be the absolute value for ink surface area on a tip with a 15 nm radius of curvature, inkjet printing for both the  $\text{Si}_x\text{N}_y$  tips and surface were carried out in a consistent manner to maximally reflect the relative trends. For four to seven droplets of MHA–ethanol, the crystallite heights do not increase above 100 nm, but rather, ink surface area increases and begins to plateau around four droplets (Figure 3a). The values of surface coverage in Figure 3a do not reach or exceed 100% because in a  $20 \times 20 \mu\text{m}$  scan area, the surface area increase of 100-nm high MHA crystallites is overshadowed by large areas without ink coverage.

The dependence of ink surface coverage on the number of MHA–ethanol droplets for flat  $\text{Si}_x\text{N}_y$  substrates translates to a linear relationship between the observed MHA transport rates and the surface area of the ink (Figure 3b). Unlike previous transport models for DPN, which account for constant concentration<sup>12</sup> or flux of MHA,<sup>13</sup> surface-area-dependent dissolution of material from the tip controls the transport rate. It has been shown that transport rates increase with tip contact area for tip dimensions up to  $250 \times 270 \text{ nm}$ .<sup>21</sup> Dissolution that depends on surface area has often been identified in fields ranging from drug release in pharmaceutical studies<sup>2</sup> to mineral dissolution in geophysical work.<sup>22</sup> In such settings, the effect of material solubility on dissolution is negligible because the system is far from saturation; the limiting factor is the surface area of the material, rather than its solubility. Although MHA has low solubility in water, the meniscus is saturated and constantly being depleted when the tip is engaged with an unmodified surface. The concentration gradient between MHA on the tip and the substrate SAM ensures continual removal and transport of material. The constant depletion of MHA from the meniscus in a DPN experiment is consistent with the conclusion that the

surface area of the ink on the tip is a dominant factor in determining the transport rate. The direct dependence of dissolution rate on the surface area can be captured by a modified Noyes–Whitney relationship,

$$\frac{dx}{dt} \propto A(S - x) \quad (2)$$

where  $dx/dt$  represents the rate of dissolution,  $A$  is the surface area,  $S$  is the saturated concentration of material, and  $x$  is the material concentration.<sup>23,24</sup> When there is continual material depletion (small  $x$ ), the rate of dissolution,  $dx/dt$ , is dominated by surface area,  $A$ . Because the limiting step of MHA pattern formation in typical DPN experiments involves phenomena at the tip rather than within the meniscus or on the substrate, the transport or deposition rate,  $D$ , can thus be attributed to the rate of dissolution,  $dx/dt$ .

The rate of dissolution at the tip has been broken down into two equations,

$$\left(\frac{dN}{dt}\right)_{\text{detach}} = \frac{b}{\pi a^2} \nu e^{-E_D/kT} \quad (3)$$

$$\left(\frac{dN}{dt}\right)_{\text{attach}} \approx b \left(\frac{kT}{2\pi m}\right)^{1/2} e^{-E_A/kT} C_0 \quad (4)$$

which represent the rates of thermally activated molecule detachment from and molecular collision-driven reattachment to the tip, respectively.<sup>25</sup> In these equations,  $N$  is the number of molecules,  $b$  is the effective contact area between MHA on the tip and the meniscus,  $\pi a^2$  is the footprint area of MHA ( $0.229 \text{ nm}^2$ ),<sup>16,17</sup>  $\nu$  is the effective molecule dissolution attempt frequency,<sup>26</sup>  $k$  is Boltzmann's constant,  $T$  is temperature,  $m$  is the mass of one MHA molecule ( $3.79 \times 10^{-22} \text{ g}$ ),  $C_0$  is the MHA concentration next to the tip ( $\sim 10^{-7}$ ),  $E_D$  is the activation energy for molecule detachment (0.467 eV per molecule),<sup>16</sup> and  $E_A$  is the activation energy for attachment (0.13 eV per molecule).<sup>25</sup> Furthermore, the net transport rate can be defined as:

$$\frac{dx}{dt} = \left(\frac{dN}{dt}\right)_{\text{detach}} - \left(\frac{dN}{dt}\right)_{\text{attach}} \quad (5)$$

Values for the attempt frequency,  $\nu$ , of MHA dissolution were previously unavailable except through model estimations. By using measured transport rates from the DPN experiments and surface coverage values, attempt frequencies for molecule detachment can be determined; these  $\nu$  values also reflect a relationship with the number of inked droplets. We have found that the attempt frequencies of MHA dissolution range from  $1.33 \times 10^9$  to  $4.42 \times 10^9 \text{ Hz}$ ,<sup>27</sup> three orders of magnitude below the upper limit of  $kT/h$  ( $\sim 6.1 \times 10^{12} \text{ Hz}$ , where  $h$  is Planck's constant) and are consistent with ideal models of chainlike molecule dissociation in liquids.<sup>25,28</sup> The lower value for attempt frequency relates to MHA detaching from silicon nitride; the higher value corresponds to MHA detachment from itself.

We conclude that the droplet-dependent MHA deposition rates are governed by ink surface coverage; the dissolution of ink into the meniscus is the limiting step in the entire transport process because the deposition of alkanethiols from the meniscus on the gold surface is a rapid process. This finding explains the large variation in transport rates associated with pens inked by dip-coating or inkwells<sup>29</sup> and attributes the variation to inhomogeneous ink distribution and uneven surface coverage. The considerable variation in transport rate has thus far precluded any knowledge of pen writing behavior prior to pattern formation. The use of inkjet printing to deliver precise amounts of material to designated locations not only has enabled one to predict and tailor MHA transport rates, but also makes DPN a

more consistent and controllable nanopatterning tool. These results are the first DPN experiments showing a direct relationship between amount of ink on a tip and corresponding surface area with transport rate.

**Acknowledgment.** The authors thank Mark Ratner and George Schatz for valuable discussions. C.A.M. acknowledges the Air Force Office of Scientific Research, Defense Advanced Research Projects Agency, National Science Foundation (NSF), and a National Security Science and Engineering Faculty Fellows Award for support of this work. L.R.G. thanks the NSF for a Graduate Research Fellowship.

**Supporting Information Available:** LFM image of sub-100 nm features produced by tips inked with one drop of 0.5 mM MHA–ethanol solution. AFM images of MHA drops printed on flat Si<sub>3</sub>N<sub>4</sub> substrates. This material is available free of charge via the Internet at <http://pubs.acs.org>.

## References and Notes

- (1) Piner, R. D.; Zhu, J.; Xu, F.; Hong, S. H.; Mirkin, C. A. *Science* **1999**, *283*, 661.
- (2) Danesh, A.; Connell, S. D.; Davies, M. C.; Roberts, C. J.; Tendler, S. J. B.; Williams, P. M.; Wilkins, M. J. *Pharm. Res.* **2001**, *18*, 299.
- (3) Choi, J. G.; Do, D. D.; Do, H. D. *Ind. Eng. Chem. Res.* **2001**, *40*, 4005.
- (4) Vesper, B. J.; Salaita, K.; Zong, H.; Mirkin, C. A.; Barrett, A. G. M.; Hoffman, B. M. *J. Am. Chem. Soc.* **2004**, *126*, 16653.
- (5) Noy, A.; Miller, A. E.; Klare, J. E.; Weeks, B. L.; Woods, B. W.; DeYoreo, J. J. *Nano Lett.* **2002**, *2*, 109.
- (6) Demers, L. M.; Ginger, D. S.; Park, S. J.; Li, Z.; Chung, S. W.; Mirkin, C. A. *Science* **2002**, *296*, 1836.
- (7) Gundiah, G.; John, N. S.; Thomas, P. J.; Kulkarni, G. U.; Rao, C. N. R.; Heun, S. *Appl. Phys. Lett.* **2004**, *84*, 5341.
- (8) Su, M.; Liu, X. G.; Li, S. Y.; Dravid, V. P.; Mirkin, C. A. *J. Am. Chem. Soc.* **2002**, *124*, 1560.
- (9) Salaita, K.; Wang, Y.; Mirkin, C. A. *Nat. Nanotechnol.* **2007**, *2*, 145.
- (10) Schwartz, P. V. *Langmuir* **2002**, *18*, 4041.
- (11) Manandhar, P.; Jang, J.; Schatz, G. C.; Ratner, M. A.; Hong, S. *Phys. Rev. Lett.* **2003**, *90*, 115505.
- (12) Sheehan, P. E.; Whitman, L. J. *Phys. Rev. Lett.* **2002**, *88*, 156104.
- (13) Jang, J. Y.; Hong, S. H.; Schatz, G. C.; Ratner, M. A. *J. Chem. Phys.* **2001**, *115*, 2721.
- (14) Weeks, B. L.; Vaughn, M. W.; DeYoreo, J. J. *Langmuir* **2005**, *21*, 8096.
- (15) Wang, Y.; Giam, L. R.; Park, M.; Lenhart, S.; Fuchs, H.; Mirkin, C. A. *Small* **2008**, *4*, 1666.
- (16) Jung, L. S.; Campbell, C. T. *J. Phys. Chem. B* **2000**, *104*, 11168.
- (17) Strong, L.; Whitesides, G. M. *Langmuir* **1988**, *4*, 546.
- (18) This calculation is based on a meniscus volume approximation wherein a cone (of same base and height) is subtracted from a cylinder of height and radius equaling 115 and 150 nm, respectively. MHA solubility in water at 25°C, pH ~ 5 is  $2.2 \times 10^{-5}$  mol/L on the basis of SciFinder predicted properties calculated using Advanced Chemistry Development (ACD/Labs) Software V8.14.
- (19) Nafday, O. A.; Vaughn, M. W.; Weeks, B. L. *J. Chem. Phys.* **2006**, *125*, 144703/1.
- (20) Deegan, R. D.; Bakajin, O.; Dupont, T. F.; Huber, G.; Nagel, S. R.; Witten, T. A. *Nature* **1997**, *389*, 827.
- (21) John, N. S.; Kulkarni, G. U. *J. Nanosci. Nanotechnol.* **2007**, *7*, 977.
- (22) Hodson, M. *Geochim. Cosmochim. Acta* **1998**, *62*, 3429.
- (23) King, C. *J. Am. Chem. Soc.* **1935**, *57*, 828.
- (24) Noyes, A. A.; Whitney, W. R. *J. Am. Chem. Soc.* **1897**, *19*, 930.
- (25) Weeks, B. L.; Noy, A.; Miller, A. E.; De Yoreo, J. J. *Phys. Rev. Lett.* **2002**, *88*, 255505.
- (26) House, J. E. *Principles of Chemical Kinetics*, 2nd ed.; Academic Press: Boston, 2007.
- (27) Using  $D$  values of 0.015 and 0.085  $\mu\text{m}^2/\text{sec}$  allows one to derive the range of  $v$  for 1 to 7 droplets, respectively. Dividing by the footprint of MHA, one can calculate  $dx/dr$ , the net transport rates, which are  $6.9 \times 10^4$  and  $3.9 \times 10^5$  molecules  $\text{s}^{-1}$ , respectively. Other values used for this calculation include  $b = 1413 \text{ nm}^2$ , which corresponds to the surface area of a hemisphere with a 15 nm radius, and  $T = 23 \text{ }^\circ\text{C}$ . For the surface area increase of the tip by 40% due to MHA, a value of  $b = 1978 \text{ nm}^2$  was used.
- (28) Evans, E. *Annu. Rev. Biophys. Biomol. Struct.* **2001**, *30*, 105.
- (29) Peterson, E. J.; Weeks, B. L.; De Yoreo, J. J.; Schwartz, P. V. *J. Phys. Chem. B* **2004**, *108*, 15206.

JP809061E